Crystal field parameters at the (0001) surface of rare-earth metals: an *ab initio* study

2005 J. Phys.: Condens. Matter 17 2061

(http://iopscience.iop.org/0953-8984/17/13/006)

INSTITUTE OF PHYSICS PUBLISHING JOURNAL OF PHYSICS: CONDENSED MATTER

J. Phys.: Condens. Matter **17** (2005) 2061–2072 doi:10.1088/0953-8984/17/13/006

Crystal field parameters at the (0001) surface of rare-earth metals: an *ab initio* study

F Welsch[1], **M Fähnle**[1] **and P J Jensen**[2]

[1] Max-Planck-Institut für Metallforschung, Heisenbergstraße 3, D-70569 Stuttgart, Germany
[2] Institut für Theoretische Physik, Freie Universität Berlin, Arnimallee 14, D-14195 Berlin, Germany

Received 8 November 2004, in final form 14 January 2005
Published 18 March 2005
Online at stacks.iop.org/JPhysCM/17/2061

Abstract

The modifications of the crystal field parameters A_{lm} at the (0001) surface of the rare-earth metals Tb, Dy, Ho, Er and Tm due to the surface-induced modifications of the charge density are investigated by the *ab initio* density functional electron theory. For the three outermost atomic layers the values of the parameters A_{20}, A_{40}, A_{60} and A_{66} which are nonzero for the hexagonal bulk are drastically different from the bulk values. The additional parameters A_{43} and A_{63} originating from the symmetry reduction at the surface are very large close to the surface. Altogether, the results show that for a thermodynamic calculation of the spin structure at the surface a simple broken-bond model does not suffice.

1. Introduction

Elementary rare-earth metals exhibit a variety of different spin structures in the bulk [1], e.g. ferromagnetic, conical, helical, various types of antiphase domain structures, etc. This variety of spin structures is a consequence of competing magnetic interactions [2], i.e. oscillatory exchange interactions of RKKY type, magnetocrystalline anisotropy and magnetoelastic interactions as well as dipole interactions. At a surface or at interfaces the delicate balance between these competing interactions is strongly modified, and it is expected that this has a big effect on the local spin structure.

In a pioneering paper Bohr *et al* [3] investigated for the first time the modifications of the bulk spin structure for Ho by the appearance of the two surfaces of a thin Ho slab. The ground state spin structure of hexagonal bulk Ho is a conical ordering [4] of the moments with a small ferromagnetic component along the hexagonal c axis corresponding to a cone opening angle Θ of 80°. The components in the basal plane are ferromagnetically aligned in each plane but are rotated relative to each other in successive basal planes. The orientations of the projections in the basal planes are described by the angles Φ (figure 1). The resulting magnetic structure is locked to the lattice periodicity and repeats itself after 12 hexagonal layers, respectively. The average angle of rotation is 30° but the moments in two successive planes show a pairwise

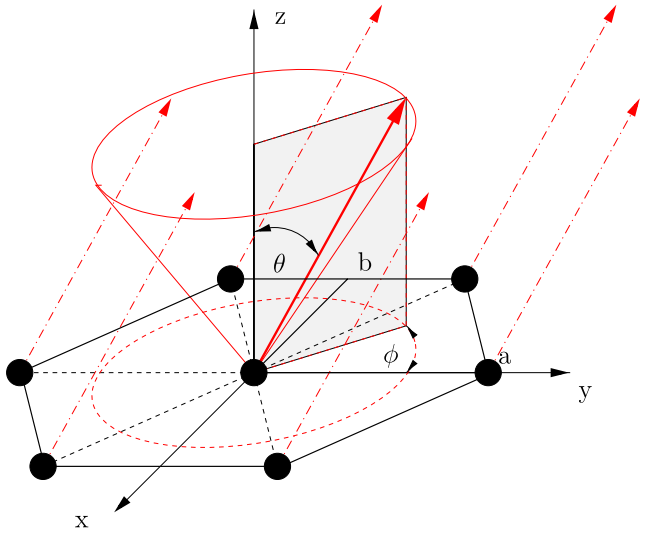

Figure 1. Definition of the cone opening angle Θ and the in-plane angle Φ describing the orientation of a magnetic moment in a hexagonal system. Note that we define Φ with respect to the *a* axis in the basal plane.

(This figure is in colour only in the electronic version)

reorientation towards the closest nearest-neighbour easy *b* axis in the plane, so that the so-called bunching angle between one of the moments and the nearest-neighbour easy *b* axis is only about 5.8° (figure 2). To determine the spin structure by theory, in general a three-step procedure is used. First, a phenomenological Hamiltonian is defined which describes the above discussed interactions in the rare-earth metal. Second, the interaction parameters appearing in this Hamiltonian are determined with the *ab initio* electron theory (as in the present paper) or by fitting the Hamiltonian to experimental results. Third, the phenomenological Hamiltonian with the so-specified interaction parameters is used in a statistical mechanics treatment (e.g. mean field theory or thermodynamic perturbation theory or exact diagonalization procedures) to determine the ground state properties and the finite-temperature properties of the spin system. To investigate by this three-step procedure the influence of the surfaces of a Ho slab on the spin structure, Bohr *et al* [3] adopted in their zero-temperature mean-field calculation the so-called broken-bond model. This means that they considered just the effect of the absence of neighbouring atoms at the surface but otherwise they used the magnetic interaction parameters of the bulk also for the surface, i.e. they did not take into account the strong modification of the electronic states at the surface [5, 6]. Within the broken-bond model they found a tendency to near-ferromagnetic alignment of the moments in the basal planes at the three or four outermost atomic layers of the slab (triplet or quartet termination). If the slab contains nine or fewer layers then the ferromagnetic state is favoured for the whole slab. More recently Leiner *et al* [7] have investigated the thickness dependence of the magnetic ordering temperature of a Ho film by the mean-field broken-bond model.

The present paper represents a first step to abandoning the broken-bond model. It has been shown by numerous calculations (see, e.g., [8–10]) within the framework of the *ab initio* density functional electron theory that, in particular, the crystal field (CF) parameters which essentially determine the magnetocrystalline anisotropy in rare-earth metals (except for Gd) depend extremely sensitively on the electronic charge density. Therefore it is the objective of

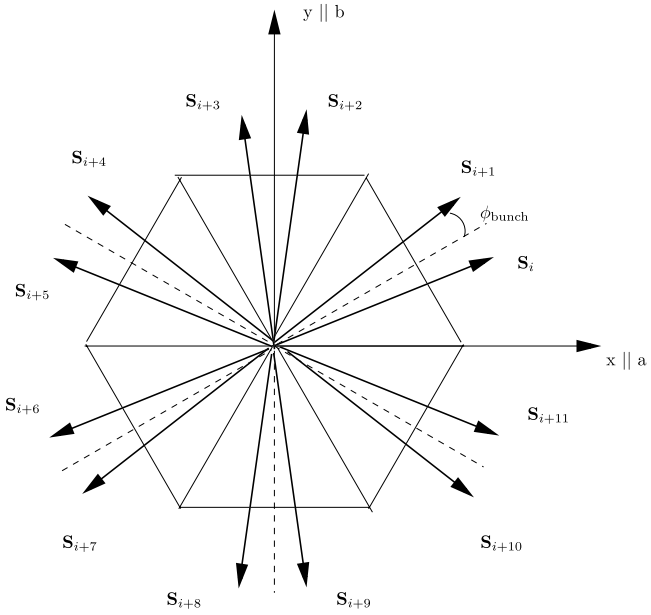

Figure 2. The ground state spin structure of bulk Ho. The figure shows the projection of the atomic moments in 12 successive (0001) layers on the basal plane. *a* and *b* denote one of the six hard and easy directions in the basal plane, respectively. Φ_{bunch} is the bunching angle.

the present paper to calculate the modification of the CF parameters near the surface by the *ab initio* electron theory. It will be shown that these modifications are very strong in the outermost three or four layers, i.e. in the regime where the broken-bond model predicts the pronounced change of the spin structure as compared to the spin structure of the bulk. This means that for a realistic determination of the spin structure at the surface the broken-bond model does not suffice.

2. Calculational method

The magnetocrystalline anisotropy energy of rare-earth (RE) metals is (except for Gd) determined by the very strong spin–orbit coupling for the 4f electrons. For many representatives of this class of materials the 4f electrons can be described by core states with a charge density $\rho_{4\text{f}}(\mathbf{r})$ which is given by the one of a free trivalent RE^{3+} ion ('standard model of RE metals', see [8, 11]). The charge density $\rho_{4\text{f}}(\mathbf{r})$ is strongly anisotropic and it interacts electrostatically with the CF produced by all the other charges in the system. The ground state orientation of the anisotropic 4f charge cloud is the one for which the energy is minimal. Rotating the 4f moments out of the ground state orientation by applying a strong oblique external magnetic field, these anisotropic charge clouds are more or less rigidly co-rotated because of the very strong spin–orbit coupling in the 4f shell. As a result, the orientation in the CF becomes less favourable, the energy increases, and this is the origin of the magnetic anisotropy energy. Hence, the 4f contribution to the magnetocrystalline anisotropy energy is obtained by calculating the expectation value of the interaction energy between the anisotropic 4f charge density of the trivalent RE^{3+} core under consideration and the density $\rho_{\text{rest}}(\mathbf{r})$ of all the other charges in the system as a function of the orientation of the 4f charge density. The anisotropic

4f charge density polarizes the charge density of the rest, and this polarization changes when the 4f charge density is rotated out of the ground state orientation, i.e. the charge density of the rest depends rather strongly on the 4f orientation [12]. However, it has been shown by a second-order perturbation theory [12, 13] that the CF parameters describing the interaction energy have to be calculated by neglecting this polarization effect, i.e. by calculating the charge density of the rest for a spherically averaged 4f charge density. The contribution V_{aniso} of the RE atom to the magnetocrystalline anisotropy energy may then be calculated from first-order thermodynamic perturbation theory based on the assumption that the exchange energy is much larger than the anisotropy energy (see [14] and references therein), yielding

$$V_{\mathrm{aniso}} = \sum_{l=1}^{6} \sum_{m=-l}^{l} A_{lm} \langle C_{lm} \rangle. \tag{1}$$

Here $\langle C_{lm} \rangle$ denotes the expectation values of the 4f multipole moments which depend on the orientation of the 4f shell and on the temperature. The quantities A_{lm} are the CF parameters. Equation (1) can be further simplified when taking into account the point symmetry of the considered RE site. For the hexagonal site of the bulk we have D_{3h} symmetry, and then the only nonzero CF parameters are A_{20}, A_{40}, A_{60} and A_{66}. Introducing a (0001) surface parallel to the hexagonal planes reduces the symmetry of the RE sites to C_{3v}, and then the nonzero CF parameters are A_{20}, A_{40}, A_{60}, A_{66} and in addition A_{43} and A_{63}.

In a simplified model [15] the A_{lm} may be determined (see above) by calculating via a multipole expansion the electrostatic interaction energy of the anisotropic 4f charge density with the aspherical charge density of all the other charges in the system (thereby neglecting the polarization of this latter charge density by the 4f shell, see above), and by representing the result in the form of equation (1). The A_{lm} are then given by:

$$A_{lm} = c_{lm} \frac{\int \mathrm{d}r\, r^2 \rho_{4\mathrm{f}}(r) V_{lm}(r)}{\int \mathrm{d}r\, r^2 \rho_{4\mathrm{f}}(r) r^n}. \tag{2}$$

Here the c_{lm} are numerical factors, $V_{lm}(r) = V_{\mathrm{ext},lm}(r) + V_{\mathrm{H},lm}[\rho_{\mathrm{rest}}]$ are the coefficients of the potential for the expansion into cubic harmonics Z_{lm}, V_{ext} is the potential of the nuclei and $V_{\mathrm{H}}[\rho_{\mathrm{rest}}]$ is the Hartree potential of the charge density ρ_{rest} of all the charges except the 4f charge density of the considered RE atom. In a more refined theory [12] based on the density functional electron theory it can be shown that there is in addition a small contribution from the exchange–correlation potential (see equation (8) of [12]) which we have taken into account in our calculations.

From equation (2) it becomes obvious that extremely accurate calculations are required for a reliable determination of the A_{lm}: the 4f charge density is localized in the interior of the atomic sphere around the considered RE atom, whereas the aspherical part of the potential (described by $V_{lm}(r)$ for $l \neq 0$) is very small in the interior and increases gradually when approaching the sphere boundary, i.e. the A_{lm} are determined by a small overlap of $\rho_{4\mathrm{f}}$ and V_{lm} which therefore has to be calculated with extreme care. In the present paper we calculated the charge densities using the density functional electron theory in local-spin-density approximation [16] (LSDA). The 4f states cannot be described correctly by the LSDA (which yields a too far extended 4f wavefunction) but we assume that for given 4f charge density $\rho_{4\mathrm{f}}$ the interaction between the 4f states and the other states via the effective potential of the density functional theory is well reproduced by the LSDA. To obtain a good approximation for the 4f charge density $\rho_{4\mathrm{f}}$ we design [8] within the standard model the 4f charge and spin density of the free RE^{3+} ion in such a way that they resemble as closely as possible the corresponding densities as obtained by a fully relativistic Dirac–Fock calculation [17], which describes the exchange–correlation effects in the 4f shell much more accurately than the LSDA. To achieve this the 4f states are

Table 1. The CF parameters $\langle r^l \rangle_{4f}\ A_{lm}$ in [K] as obtained by the FLAPW method and the FLMTO method [21].

RE	Method	$\langle r^2 \rangle_{4f}\ A_{20}$	$\langle r^4 \rangle_{4f}\ A_{40}$	$\langle r^6 \rangle_{4f}\ A_{60}$	$\langle r^6 \rangle_{4f}\ A_{66}$
Tb	FLAPW	−164	19.0	2.48	21.8
	FLMTO	−194	17.4	2.38	21.1
Dy	FLAPW	−163	17.5	2.60	22.4
	FLMTO	−200	16.1	2.52	21.9
Ho	FLAPW	−153	14.9	2.39	20.5
	FLMTO	—	—	—	—
Er	FLAPW	−138	13.3	2.31	19.8
	FLMTO	−170	11.9	2.24	19.4
Tm	FLAPW	−105	10.9	2.14	18.2
	FLMTO	−142	9.45	1.85	16.0

calculated by the LSDA in a localization sphere with the restriction that the 4f wavefunctions drop to zero at the sphere boundary. The radius of the localization sphere is chosen in such a way that the so-obtained expectation values $\langle r^l \rangle_{4f}$ are as close as possible to the respective expectation values of the Dirac–Fock calculation for the free trivalent RE^{3+} ion. For the RE metals this is obtained for a localization radius which is identical to the muffin-tin radius for touching muffin-tin spheres. Because the tails of the 4f states beyond the localization sphere are cut in this procedure, we neglect any contribution to the CF parameters arising from the overlap of the real 4f charge density and the aspherical part of the potential outside the localization sphere. Because V_{6m} increases most strongly when approaching the muffin-tin sphere we expect that the calculated CF parameters for $l = 6$ exhibit the largest uncertainties. In the present paper the valence states are obtained by the WIEN97 code [18], which is based on the full-potential linearized-augmented-plane-wave (FLAPW) method [19]. Spurious 4f valence contributions due to the deficiency of the LSDA to describe correctly 4f states are thereby removed by choosing negative 4f augmentation energies, see [8]. The polarization of the non-4f core states by the surroundings has been taken into account by a method described in [20].

3. *Ab initio* results for the crystal-field parameters

As a test for our FLAPW calculations we first determined the CF parameters for bulk Tb, Dy, Ho, Er and Tm and compared our results with those of corresponding former calculations [21] within the framework of the full-potential linear-muffin-tin-orbital method (FLMTO). As shown in table 1, the agreement between the results of the two calculations is satisfactory in view of the fact that the CF parameters depend extremely sensitively on the charge densities.

The layer-dependent CF parameters of a slab were calculated by a supercell method. Thereby a layer consisting of 16 basal planes in hcp stacking and a vacuum sheet on top is repeated periodically. By test calculations we showed that a vacuum sheet of thickness $d_{vac} = 2c$ is sufficient to neglect the interaction effects of the RE layers across the vacuum sheet. For the lattice parameters c and a we inserted the experimental values. We performed two types of calculation. In the first calculation the atoms in the slab are in the positions they would have in a bulk material. In a second calculation we determined for Tb and Ho by the FLAPW calculation the actual positions of the atoms in the slab by allowing for relaxations of the interplane distances (figure 3).

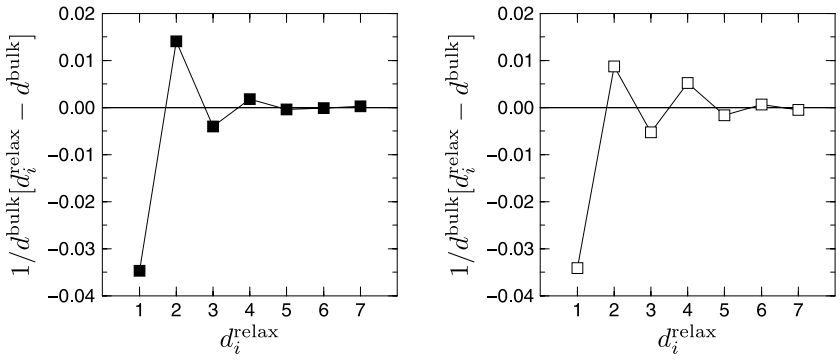

Figure 3. Modifications of the interlayer distances in a 16-layer slab of Tb (left) and Ho (right). The quantity d_i^{relax} is the distance between layer i and layer $i + 1$ (layer 1 denotes the outermost layer), and d^{bulk} is the interlayer distance in the bulk material.

The results for the layer-dependent CF parameters from the calculation without (with) relaxation are given in table 2 (table 3). By comparing the results of the two tables we can investigate the influence of structural relaxations on the CF parameters. There are strong modifications of the respective bulk values for the first three to four layers which are especially strong for A_{20} which is a factor of more than two larger at the surface than in the bulk. Furthermore, it is remarkable that in all considered materials the CF parameter A_{40} is negative at the surface, whereas it is positive in the bulk. This changes when allowing for interlayer relaxations (table 3, figures 4 and 5). Then the surface value of A_{40} is again positive as in the bulk, at least for Tb and Ho for which the relaxations have been performed.

It is possible to rewrite equation (2) as a relation between the CF parameters and the charge densities $\rho_{4\mathrm{f}}$ and ρ, where ρ denotes the density of all the charges except for the charges of the considered 4f shell. Then it is possible to subdivide the total CF parameter into a valence contribution which is related to the part of the charge density $\rho(r)$ which is located in the muffin-tin sphere of the considered 4f shell, and a lattice contribution arising from the charge density outside. In the classical point-charge model only the lattice contribution is taken into account, whereby the corresponding charge density is modelled by an assembly of fictitious point charges. It has been shown [8, 9, 15] that this point-charge model is totally inappropriate for RE metals. For instance, in the series $RECo_5$ the valence and lattice contributions to A_{20} are [8] of about the same size but opposite in sign so that the total CF parameter A_{20} is much smaller in size than the two contributions. It is, of course, interesting to analyse the CF parameters of the elementary RE metals also in this line and to investigate the effect of the symmetry breaking at the surface on the two contributions. As shown in figure 6 for the case of Ho (similar results are obtained for all considered RE metals) the CF parameter A_{20} of the bulk is strongly dominated by the negative lattice contribution (in contrast to the situation found for the series $RECo_5$, see above). At the surface the valence contribution becomes strongly negative and dominates the lattice contribution which is now positive. The strong modification of the valence contribution is totally inconsistent with a broken-bond model in which it is assumed that the charge densities of the remaining atoms are conserved when removing the upper part of the crystal upon creation of the surface. In that simple model the valence contribution would not be modified at the surface. For the other CF parameters the valence contribution is mostly larger than the lattice contribution both in the bulk and at the surface and has a sign opposite to the sign of the lattice contribution. Upon interlayer relaxation the valence contribution at the surface changes sometimes more strongly than the

Table 2. The layer-dependent CF parameters $\langle r^l \rangle_{4f}\ A_{lm}$ in [K] as obtained for a slab consisting of 16 basal planes in hcp stacking. The symbols SF, L_i and B denote the outermost layer ('surface', $i = 1$), the layer i and the innermost layer ('bulk', $i = 8$). The atoms are in the positions they would have in the corresponding bulk material.

RE	KFP	SF	L_2	L_3	L_4	L_5	L_6	L_7	B
Tb	$\langle r^2 \rangle_{4f}\ A_{20}$	−409	−72	−230	−160	−177	−164	−161	−166
	$\langle r^4 \rangle_{4f}\ A_{40}$	−2.2	13.2	21.2	17.4	19.3	18.5	18.8	18.9
	$\langle r^4 \rangle_{4f}\ A_{43}$	−433	−258	20.6	12.4	12.7	4.0	0.7	2.56
	$\langle r^6 \rangle_{4f}\ A_{60}$	1.65	2.45	2.37	2.43	2.41	2.42	2.42	2.42
	$\langle r^6 \rangle_{4f}\ A_{63}$	17.0	1.4	−0.1	−0.1	0	0	0	0
	$\langle r^6 \rangle_{4f}\ A_{66}$	20.3	21.3	21.5	21.3	21.5	21.5	21.5	21.5
Dy	$\langle r^2 \rangle_{4f}\ A_{20}$	−356	−81	−225	−161	−174	−156	−161	−166
	$\langle r^4 \rangle_{4f}\ A_{40}$	−2.8	14.0	18.1	16.7	17.6	17.1	17.3	17.4
	$\langle r^4 \rangle_{4f}\ A_{43}$	−385	−257	−7.3	5.8	7.8	2.4	1.4	2.1
	$\langle r^6 \rangle_{4f}\ A_{60}$	1.76	2.56	2.52	2.56	2.55	2.56	2.56	2.56
	$\langle r^6 \rangle_{4f}\ A_{63}$	18.0	1.4	0	−0.1	0	0	0	0
	$\langle r^6 \rangle_{4f}\ A_{66}$	20.8	22.1	22.3	22.0	22.2	22.2	22.2	22.2
Ho	$\langle r^2 \rangle_{4f}\ A_{20}$	−297	−86	−187	−142	−155	−143	−147	−146
	$\langle r^4 \rangle_{4f}\ A_{40}$	−6.9	14.5	14.2	15.2	14.9	15.1	15.0	15.1
	$\langle r^4 \rangle_{4f}\ A_{43}$	−327	−230	−30	−8.6	−4.8	−1.1	−1.3	0.3
	$\langle r^6 \rangle_{4f}\ A_{60}$	1.63	2.32	2.32	2.33	2.32	2.33	2.33	2.33
	$\langle r^6 \rangle_{4f}\ A_{63}$	16.4	1.2	0	0.1	0	0	0	0
	$\langle r^6 \rangle_{4f}\ A_{66}$	18.6	20.1	20.3	19.9	20.1	20.1	20.0	20.1
Er	$\langle r^2 \rangle_{4f}\ A_{20}$	−253	−105	−152	−133	−131	−126	−128	−127
	$\langle r^4 \rangle_{4f}\ A_{40}$	−11.5	14.1	10.9	13.5	12.3	13.1	12.8	12.9
	$\langle r^4 \rangle_{4f}\ A_{43}$	−264	−195	−33.5	−10.8	−9.0	−5.3	−1.6	−1.0
	$\langle r^6 \rangle_{4f}\ A_{60}$	1.58	2.22	2.24	2.24	2.24	2.24	2.24	2.24
	$\langle r^6 \rangle_{4f}\ A_{63}$	15.7	1.0	0	−0.1	0	0	0	0
	$\langle r^6 \rangle_{4f}\ A_{66}$	17.9	19.3	19.4	19.1	19.2	19.1	19.1	19.1
Tm	$\langle r^2 \rangle_{4f}\ A_{20}$	−211	−122	−101	−103	−91	−92	−83	−85
	$\langle r^4 \rangle_{4f}\ A_{40}$	−15.2	12.5	7.9	11.5	9.7	10.2	10.2	10.2
	$\langle r^4 \rangle_{4f}\ A_{43}$	−190	−152	−29	−9.0	0.3	−3.6	2.3	−1.5
	$\langle r^6 \rangle_{4f}\ A_{60}$	1.49	2.07	2.10	2.08	2.08	2.07	2.07	2.07
	$\langle r^6 \rangle_{4f}\ A_{63}$	14.6	0.8	0	0	−0.1	0	0	0
	$\langle r^6 \rangle_{4f}\ A_{66}$	16.8	18.0	17.9	17.8	17.6	17.5	17.6	17.5

lattice contribution, and the strong modification of the valence contribution is responsible for the change in sign of A_{40} upon relaxation (table 3).

The complete failure of the broken-bond model becomes apparent from the fact that the additional CF parameters A_{43} and A_{63}, which originate from the symmetry reduction at the surface and which are neglected in a broken-bond model, are in fact very large for the layers close to the surface. For example, for the surface layer of Ho we have $\langle r^4 \rangle_{4f}\ A_{40} = -6.9$ K but $\langle r^4 \rangle_{4f}\ A_{43} = -329$ K, or $\langle r^6 \rangle_{4f}\ A_{60} = 1.63$ K but $\langle r^6 \rangle_{4f}\ A_{63} = 16.4$ K. This again clearly demonstrates that the surface-induced modification of the charge densities can by no means be neglected when calculating the CF parameters. This means that for a realistic description of the spin structure at the surface by the three-step procedure discussed above, the broken-bond model for the interaction parameters appearing in the phenomenological Hamiltonian does not suffice, and one must use layer-dependent parameters.

Table 3. The layer-dependent CF parameters $\langle r^l \rangle_{4f}\ A_{lm}$ in [K] for the outermost layer of a 16-layer slab from the calculation without (nr) and with (r) interlayer relaxation. The table gives the total CF parameters and the respective valence and lattice contributions.

	Terbium		Holmium	
SF	nr	r	nr	r
$\langle r^2 \rangle_{4f}\ A_{20}$	−390	−388	−295	−291
$\langle r^2 \rangle_{4f}\ A_{20}^{val}$	−619	−552	−487	−422
$\langle r^2 \rangle_{4f}\ A_{20}^{Gitter}$	229	164	192	131
$\langle r^4 \rangle_{4f}\ A_{40}$	−2.2	4.5	−6.8	2.9
$\langle r^4 \rangle_{4f}\ A_{40}^{val}$	14.8	24.7	−5.9	11.4
$\langle r^4 \rangle_{4f}\ A_{40}^{Gitter}$	−17.0	−20.2	−0.9	−8.5
$\langle r^4 \rangle_{4f}\ A_{43}$	−435	−375	−328	−277
$\langle r^4 \rangle_{4f}\ A_{43}^{val}$	−1113	−996	−860	−858
$\langle r^4 \rangle_{4f}\ A_{43}^{Gitter}$	678	621	532	581
$\langle r^6 \rangle_{4f}\ A_{60}$	1.73	1.87	1.61	1.73
$\langle r^6 \rangle_{4f}\ A_{60}^{val}$	3.59	3.91	3.20	3.38
$\langle r^6 \rangle_{4f}\ A_{60}^{Gitter}$	−1.86	−2.04	−1.47	−1.65
$\langle r^6 \rangle_{4f}\ A_{63}$	17.1	20.3	16.2	19.2
$\langle r^6 \rangle_{4f}\ A_{63}^{val}$	48.3	49.8	40.1	42.0
$\langle r^6 \rangle_{4f}\ A_{63}^{Gitter}$	−31.2	−29.5	−23.9	−22.8
$\langle r^6 \rangle_{4f}\ A_{66}$	21.5	21.3	18.3	18.2
$\langle r^6 \rangle_{4f}\ A_{66}^{val}$	51.4	52.8	39.2	41.0
$\langle r^6 \rangle_{4f}\ A_{66}^{Gitter}$	−29.9	−31.5	−20.9	−22.8

4. Conclusions

In the present paper we have shown by means of the *ab initio* density functional electron theory that the modification of the charge density close to the surface of a rare-earth metal has a very strong effect on the values of the CF parameters A_{lm}. Those CF parameters which are nonzero in the hexagonal bulk (A_{20}, A_{40}, A_{60}, A_{66}) are strongly modified for the three to four outermost layers. There are additional nonzero CF parameters A_{43} and A_{63} due to the symmetry reduction at the surface, which exhibit very large values close to the surface. Altogether, this means that a broken-bond model (which considers just the effect of the absence of the neighbouring atoms at the surface, but uses for the remaining magnetic interaction parameters the bulk values) fails badly.

Originally we had in mind to explore the spin structure of Ho close to the surface by the three-step approach discussed in the introduction, thereby adopting the broken-bond model for the exchange interactions, but going beyond the broken-bond model for the CF parameters by using our *ab initio* calculated layer-dependent values in the phenomenological Hamiltonian for the statistical mechanics calculations. The objective was to investigate the influence of the modifications of the CF parameters on the near-surface spin structure, and to compare the near-surface spin structure with the bulk spin structure. As a first step, we calculated the ground-state bulk spin structure by the first order thermodynamic perturbation theory [14, 22] (including the effect of dipolar interactions), thereby using the exchange couplings and the CF parameters (table 4) as given in [23]. Our results agreed well with those obtained in [23] by an exact

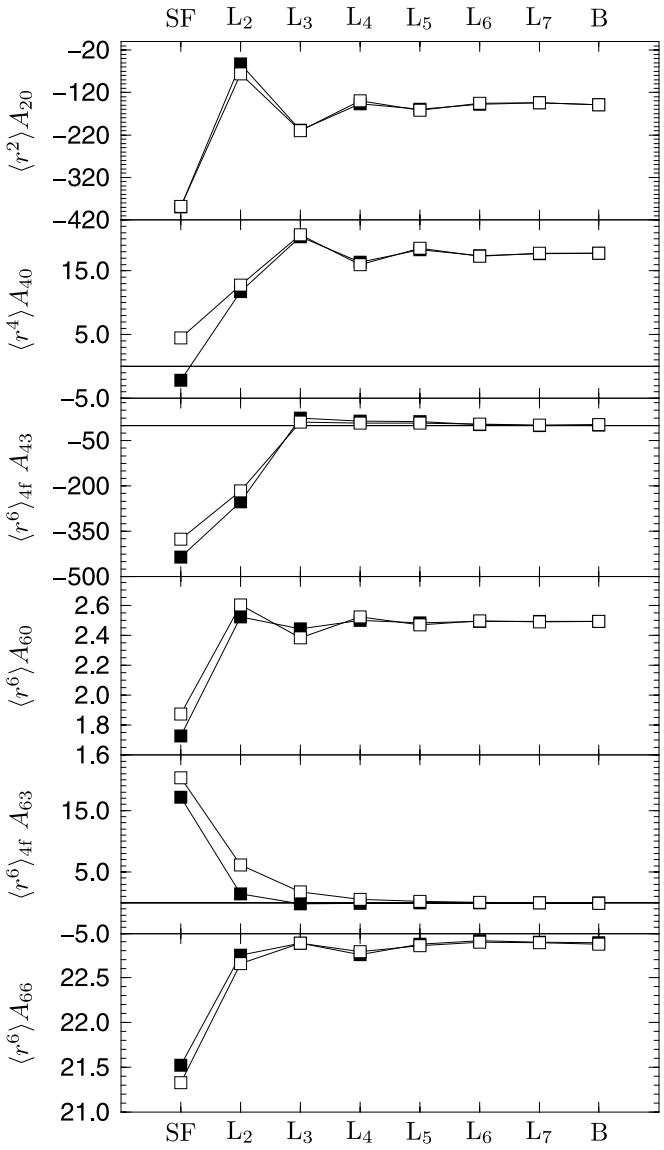

Figure 4. The layer-dependent CF parameters in [K] for Tb from a calculation without (full squares) and with (open squares) interlayer relaxations. The symbols SF, L_i and B denote the outermost layer, the layer i and the innermost layer of the 16-layer slab.

diagonalization of the corresponding mean-field Hamiltonian. We obtained a cone opening angle of 71.6° and a bunching angle of 7°. The sole action of the exchange couplings would thereby lead to a helical ground-state spin structure confined to the basal plane (corresponding to a cone opening angle of 90°). The action of A_{66} is responsible for the bunching of the moments in the basal plane [22], and the combined action of A_{20}, A_{40}, A_{60} and the dipolar interactions is responsible [24] for the development of a cone opening angle different from 90°. When using our *ab initio* calculated CF parameters, however, we obtained the helical structure in the basal plane with a bunching angle of 11.6° which is about twice the experimental value.

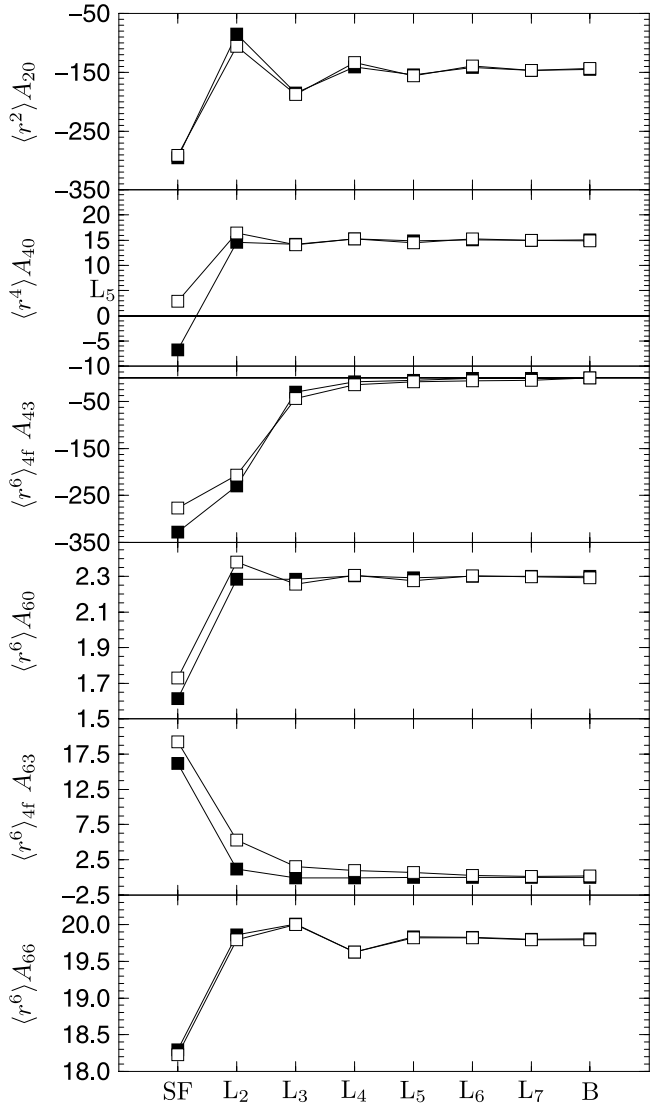

Figure 5. The layer-dependent CF parameters in [K] for Ho from a calculation without (full squares) and with (open squares) interlayer relaxations. The symbols SF, L_i and B denote the outermost layer, the layer i and the innermost layer of the 16-layer slab.

The reason for these artefacts is that our calculated values of $\langle r^6\rangle_{4f}\ A_{60}$ and $\langle r^6\rangle_{4f}\ A_{66}$ are a factor of about four smaller than the values used in [23] (see table 4). As outlined in section 2 we indeed expect that the calculated CF parameters for $l = 6$ exhibit the largest uncertainty. Because the calculated CF parameters did not yield the correct ground-state spin structure for the bulk, we refrained from investigating the influence of the near-surface modifications of the CF parameters on the spin structure. Of course we are nevertheless convinced that our *ab initio* calculations yield at least semiquantitative results for the modifications of the CF parameters at the surface, and the investigation of these modifications was the main objective of the present paper.

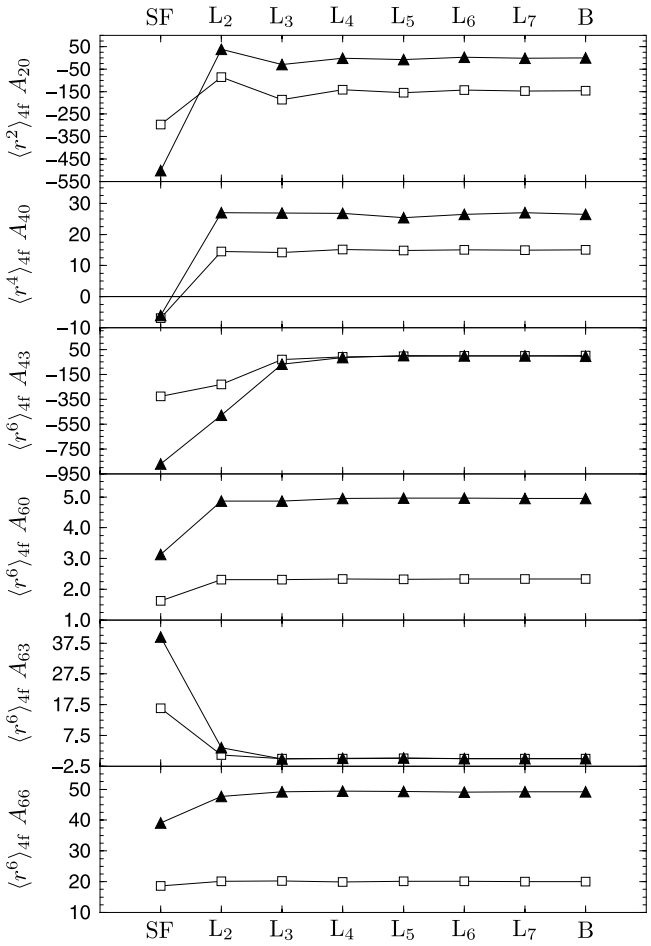

Figure 6. The total (open squares) layer-dependent CF parameters in [K] for Ho from the non-relaxed calculation as well as the respective valence contributions (full triangles). The symbols SF, L_i and B denote the outermost layer, the layer i and the innermost layer of the 16-layer slab, respectively.

Table 4. The values in [K] of the CF parameters $\langle r^l \rangle_{4f}\ A_{lm}$ for bulk Ho as used in [23], in comparison with our *ab initio* values.

	$\langle r^2 \rangle_{4f}\ A_{20}$	$\langle r^4 \rangle_{4f}\ A_{40}$	$\langle r^6 \rangle_{4f}\ A_{60}$	$\langle r^6 \rangle_{4f}\ A_{66}$
Ref. [23]	−125	0.0	8.52	84.3
Ab initio	−153	14.9	2.39	20.5

Acknowledgments

This work was supported by the Deutsche Forschungsgemeinschaft (DFG) under Project No. FA 196/8-2. P J Jensen acknowledges support from the DFG, SfB-290, TPA01.

References

[1] Koehler W C 1965 *J. Appl. Phys.* **36** 1078
[2] Kronmüller H and Schmidt W 1975 *Physica* B **80** 330
[3] Bohr J, Gibbs D, Axe J D, Moncton D E, d'Amico K L, Majkrzak C F, Kwo J, Hong M, Chien C L and Jensen J 1989 *Physica* B **159** 93
[4] Koehler W C, Cable J W, Child H R, Wilkinson M K and Wollan E O 1967 *Phys. Rev.* **158** 450
[5] Wu R Q, Li C, Freeman A J and Fu C L 1991 *Phys. Rev.* B **44** 9400
[6] Li D Q, Hutchings C W, Dowben P A, Hwang C, Wu R T, Onellion M, Andrews A B and Erskine J L 1991 *J. Magn. Magn. Mater.* **99** 85
[7] Leiner V, Ay M, Schmitte T, Zabel H, Weschke E, Ott H, Schierle E, Schüssler-Langeheine C, Vyalikh D V, Kaindl G and Jensen P J 2004 *Phys. Rev. Lett.* **93** 157204
[8] Hummler K and Fähnle M 1996 *Phys. Rev.* B **53** 3272
[9] Richter M 1998 *J. Phys. D: Appl. Phys.* **31** 1017
[10] Fähnle M and Welsch F 2002 *Physica* B **321** 198
[11] Brooks M S S and Johansson B 1993 *Handbook of Magnetic Materials* ed K H J Buschow (New York: Elsevier Science) p 139
[12] Buck S and Fähnle M 1997 *J. Magn. Magn. Mater.* **166** 297
[13] Fähnle M and Buck S 1998 *Phys. Rev. Lett.* **80** 4107
[14] Millev Y and Fähnle M 1995 *Phys. Rev.* B **52** 4336
Millev Y and Fähnle M 1995 *Phys. Rev.* B **51** 2937
[15] Coehoorn R 1991 *Supermagnets, Hard Magnetic Materials* (*NATO Advanced Study Institute, Series C* vol 331) ed G J Long and F Grandjean (Dordrecht: Kluwer) p 133
[16] Perdew J P and Wang Y 1992 *Phys. Rev.* B **45** 13244
[17] Freeman A J and Desclaux J P 1979 *J. Magn. Magn. Mater.* **12** 11
[18] Blaha P, Schwarz K, Sorantin P and Trickey S B 1990 *Comput. Phys. Commun.* **59** 399
[19] Wimmer E, Krakauer H, Weinert M and Freeman A J 1981 *Phys. Rev.* B **24** 864
[20] Ehmann J and Fähnle M 1997 *Phys. Rev.* B **55** 7478
[21] Buck S 1998 *PhD Thesis* University of Stuttgart
[22] Jensen J and Mackintosh A R 1991 *Rare Earth Magnetism: Structures and Excitations* (New York: Oxford Science Publications)
[23] Jensen J 1996 *Phys. Rev.* B **54** 4021
[24] Larsen C C, Jensen J and Mackintosh A R 1987 *Phys. Rev. Lett.* **59** 712